International Journal of Chemical, Materials and Biomolecular Sciences
ISSN: 2415-6620
Vol:8, No:12, 2014

# Low-Temperature Luminescence Spectroscopy of Violet Sr-Al-O:$Eu^{2+}$ Phosphor Particles

Keiji Komatsu, Hayato Maruyama, Ariyuki Kato, Atsushi Nakamura, Shigeo Ohshio, Hiroki Akasaka, Hidetoshi Saitoh

***Abstract*—**Violet Sr–Al–O:$Eu^{2+}$ phosphor particles were synthesized from a metal–ethylenediaminetetraacetic acid (EDTA) solution of Sr, Al, Eu, and particulate alumina via spray drying and sintering in a reducing atmosphere. The crystal structures and emission properties at 85–300 K were investigated. The composition of the violet Sr–Al–O:$Eu^{2+}$ phosphor particles was determined from various Sr–Al–O:Eu2+ phosphors by their emission properties' dependence on temperature. The highly crystalline $SrAl_{12}O_{19}$:$Eu^{2+}$ emission phases were confirmed by their crystallite sizes and the activation energies for the 4f5d–$^8S_{7/2}$ transition of the $Eu^{2+}$ ion. These results showed that the material identification for the violet Sr–Al–O:$Eu^{2+}$ phosphor was accomplished by the low-temperature luminescence measurements.

***Keywords*—**Low temperature luminescence spectroscopy, Material Identification, Strontium aluminates phosphor.

## I. Introduction

MANY researchers are attracted to Sr–Al–O-related crystals for their functions as long-phosphorescence light-induced phosphors, thermal-induced phosphors, and stress-induced phosphors [1]-[6]. In particular, $Eu^{2+}$-doped Sr–Al–O:$Eu^{2+}$ phosphors have high chemical stabilities, high emission brightness, and long afterglow properties. The emission colors of the Sr–Al–O:$Eu^{2+}$ phosphors depend on their crystal structures and stoichiometries [7]. The electron configuration of the emission center, the $Eu^{2+}$ ion, also depends on these parameters. The energy level of the 5d electron in the $Eu^{2+}$ ion affects the crystal field strongly. Therefore, the energy level of $(4f)^6(5d)^1$ depends on the strength of the crystal-field effects [8]. As a result, the Sr–Al–O:$Eu^{2+}$ phosphors are known as one of the phosphor materials that are tunable from violet to green [8].

Synthesis of the 410-nm violet Sr–Al–O:$Eu^{2+}$ phosphor using elemental diffusion from exogenous material has also been reported [9]. This method requires that sintering be performed under a reducing atmosphere, starting with Sr–Al–O:Eu powder with the molar ratio of 6.86:8:0.14 for Sr:Al:Eu complexed with ethylenediaminetetraacetic acid (EDTA). Metal oxide powder from metal-EDTA complex is suitable for phosphor materials design because of homogenous compositionally [10]-[11]. Advantages of EDTA route synthesis were confirmed by Y-B-C-O compounds film's synthesis from EDTA complexes [12] The emission of the product was dependent on the degree of elemental Al diffusion from the alumina substrate, which was controlled by varying the sintering conditions. Furthermore, the synthesis of Sr–Al–O:$Eu^{2+}$ phosphor particles using elemental Al diffusion was developed to fabricate particles with superior properties for commercial applications in paints, for example [13] Instead of a polycrystalline alumina plate, the 405 nm violet emission phase was found in a 1-μm-thick coating layer covering the Sr–Al–O:$Eu^{2+}$ particles. These violet emission phases were formed in the alumina. Some Sr–Al–O crystalline phases were then formed on the surface area by elemental Al diffusion from the alumina. The seven Sr–Al–O crystalline phases—$SrAl_2O_4$, $SrAl_{12}O_{19}$, $Sr_2Al_6O_{11}$, $Sr_3Al_2O_6$, $Sr_4Al_{14}O_{25}$, $Sr_7Al_{12}O_{25}$, $Sr_9Al_6O_{18}$—were contained. From a stand point of phosphor material design, it is important to improve its emission properties in order to determine the crystal structure and stoichiometries for the violet Sr–Al–O crystalline phase.

The emission behavior and properties such as emission wavelength and emission peak width of the $Eu^{2+}$-doped phosphor material are strongly affected by its surrounding temperature [14]-[17]. Emission processes at 300 K include the thermal deactivation process, whose effect can be reduced by decreasing the sample's temperature to 300 K or lower. The thermal deactivation process originates from lattice vibrations in the crystal. For example, $Ca_{0.8}Sr_{0.2}S$ phosphor shows a shorter emission wavelength with increasing temperature. This phenomenon is explained by a larger number of electrons located in the higher excited energy level of the $Eu^{2+}$ ion that is associated with increasing temperature. Next, the phosphor material undergoes lattice expansion, forming a longer emission center–ligand distance (e.g., $Eu^{2+}$–$S^{2-}$) as the temperature increases. The electrostatic interaction in the crystal field at 300 K then becomes weaker than that at lower temperatures. In contrast, the number of electrons that are located in the higher excited energy level of $Eu^{2+}$ ion tends to decrease at low temperatures, and the electrons in the crystal can become isolated and localized. The emission properties of phosphor materials are affected strongly by temperature because of phonon effects; they are also independent of the material composition of the phosphors themselves at low temperature. The minimum thermal energy required for an

K Komatsu, A. Kato, S. Ohshio and H. Saitoh are with the Nagaoka Univeristy of Technology, 1603-1 Kamitomioka-Machi, Nagaoka, Niigata, Japan (phone: +81-258-47-9342; fax: +81-258-47-9300, e-mail: Keiji_Komatsu@mst.nagaokaut,ac.jp).

H. Maruyama and H. Akasaka were with the Nagaoka Univeristy of Technology, 1603-1 Kamitomioka-Machi, Nagaoka, Niigata, Japan (e-mails: Hayato_Maruyama@mst.nagaokaut.ac.jp and akasaka@mech.titech.ac.jp).

A. Nakamura is with the Chubu Chelest Co., Ltd., 3-3-3 Hinagahigashi, Yokkaichi, Mie 510-0886, Japan and also with the Nagaoka Univeristy of Technology, 1603-1 Kamitomioka-Machi, Nagaoka, Niigata, Japan as visiting associate professor (phone:+81-59-346-2840, e-mail: nakamura_a@chubuchelest.co.jp).

electron to hop between levels in the crystal can be estimated by the Arrhenius equation [18], [19]. In $Eu^{2+}$-doped phosphor material, the estimated thermal energy is related to transitions from the $^6P_{7/2}$ (minimum excited energy level) to $4f^65d^1$ level of the $Eu^{2+}$ ion. Material identification of the Sr–Al–O:$Eu^{2+}$ phosphors from the low-temperature luminescence properties is therefore possible based on transition rules for the $Eu^{2+}$ ion compared to its properties at room temperature.

In this study, material identification was performed on the violet Sr–Al–O:$Eu^{2+}$ phosphor particles synthesized using elemental Al diffusion. At room temperature, both $SrAl_{12}O_{19}$:$Eu^{2+}$ and $Sr_7Al_{12}O_{25}$:$Eu^{2+}$ exhibit violet luminescence at 410 nm. Identification of the violet Sr–Al–O:$Eu^{2+}$ phosphor particles was conducted through luminescence spectroscopy measurements at low temperature to determine the crystalline structure and emission properties at 85–300 K. The results were compared to the reported emission properties of Sr–Al–O:$Eu^{2+}$ single crystals at 85–300K. In addition, the crystallite diameter size and activation energy of the Sr–Al–O:$Eu^{2+}$ phosphor particles were estimated from X-ray diffraction (XRD) patterns and cathodoluminescence (CL) spectra to study the relationship between crystalline degrees and 4f5d–$^8S_{7/2}$ transition efficiency.

## II. Experimental Method

### A. Materials

Fig. 1 shows a schematic diagram showing the preparation of a sample, including dispersion of alumina in the (Sr, Al, Eu)–EDTA solution made from Sr–EDTA solution, Eu–EDTA solution, and EDTA–Al–$NH_4$ crystals. Three EDTA complexes, Sr–, Al–, and Eu–EDTA, were prepared for the synthesis of Sr–Al–O:$Eu^{2+}$ phosphor particles. A colorless Sr–EDTA aqueous solution was prepared by reacting $SrCO_3$, EDTA•2H•2$NH_4$, and purified water by stirring them together for 30 min at 80ºC. A pale pink Eu–EDTA aqueous solution was also prepared by reacting $Eu_2O_3$, EDTA•2H•2$NH_4$, and purified water by stirring them together for 2 h at 100ºC.

### B. Experiment

To produce the Sr–Al–O:$Eu^{2+}$ phosphor particles, particulate alumina (average particle size: 1.0 μm; Brunauer–Emmett–Teller (BET) surface area: 5.0 $m^2/g$) (A-43-M, Showa Denko K. K.) was dispersed in the (Sr, Al, Eu)–EDTA solution and then spray dried using a spray drier (SD-1000, Tokyo Rikakikai Co., Ltd.). The resulting mixture was sintered in a muffle furnace for 3 h at 800°C and then placed in a reducing atmosphere for 1 h at 1400–1500°C. A schematic outline of the process for sample preparation is shown in Fig. 1. Three samples of Sr–Al–O:$Eu^{2+}$ phosphor particles were obtained and the sintering temperature of each is shown in Table I.

The emission properties of the samples were analyzed by photoluminescence spectroscopy (JASCO FP-6500). X-ray diffractometry (XRD; M03XHF and MXP3, Mac Science) was conducted to determine the crystal structure. Crystallite diameters of the Sr–Al–O:$Eu^{2+}$ phosphor particles were calculated from the Scherrer equation. The form factor, K, was constant at K = 9. The temperature dependence of the emission properties at 85–300 K was analyzed by cathodoluminescence (CL) microscopy (MonoCL3, Gatan Inc.). The accelerating voltage was 30 kV. The sample was mounted on the stage of the scanning electron microscope (SEM; JSM T300, JEOL) equipped with an external liquid-nitrogen delivery system for cooling. The temperature of the sample was controlled by a temperature controller (E5CK, Omron). Cathodoluminescence from the sample was passed through a built-in light-focusing system and then through an optical fiber (STU200D/10, Itami) coupled to a monochromator (Cornerstone 130, Oriel Instruments) and a photomultiplier (R928, Hamamatsu Photonics K. K.). The spectra were plotted after correcting the spectral sensitivity of the detection system [20]. The activation energy, *Ea*, for the Sr–Al–O:$Eu^{2+}$ particles were calculated from the CL intensities (I) for each sample using the Arrhenius relationship, $I = A \cdot \exp(-Ea/k \cdot 1/T)$. Then, A is frequency factor, independent of the temperature, and k is the Boltzman constant. Using the relationship $[\log(I) = -E_a/k \cdot 1/T + \log A]$, $\log(I)$ was then plotted against 1/T. The activation energies of the Sr–Al–O:$Eu^{2+}$ phosphor particles were estimated from the gradients of these plots.

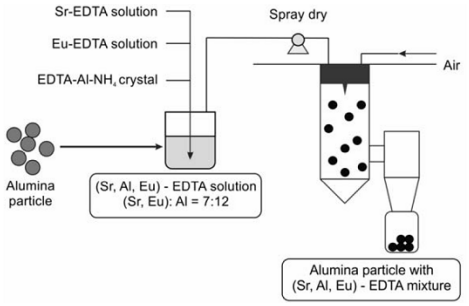


Fig. 1 Schematic diagram showing the preparation of a sample, including dispersion of alumina in the (Sr, Al, Eu)–EDTA solution made from Sr–EDTA solution, Eu–EDTA solution, and EDTA–Al–$NH_4$ crystals

TABLE I
Sintering Temperatures of the Sr-Al-O:$Eu^{2+}$ Phosphor Particles

| Sample ID | Sintering temperature (°C) |
|---|---|
| Sample 1 | 1400 |
| Sample 2 | 1450 |
| Sample 3 | 1500 |

## III. Results and Discussion

XRD measurements were conducted to identify the crystal structure of the Sr–Al–O:$Eu^{2+}$ phosphor particles obtained. Fig. 2 shows the XRD patterns of the Sr–Al–O:$Eu^{2+}$ phosphor particles. The assignments of the XRD peaks are based on the International Centre for Diffraction Data (ICDD) data card. All Sr–Al–O:$Eu^{2+}$ phosphor particles contained the Sr–Al–O crystalline phases $SrAl_2O_4$, $SrAl_{12}O_{19}$, $Sr_2Al_6O_{11}$, $Sr_3Al_2O_6$, $Sr_4Al_{14}O_{25}$, $Sr_7Al_{12}O_{25}$, and $Sr_9Al_6O_{18}$; all Sr–Al–O:$Eu^{2+}$ phosphor particles also exhibited some diffraction patterns of $Al_2O_3$, which was used as an elemental diffusion source. These

results showed that the Sr–Al–O:$Eu^{2+}$ phosphor particles obtained in the study contained the seven types of Sr–Al–O:$Eu^{2+}$ crystalline phases and related materials, and these phases coexisted in the samples.

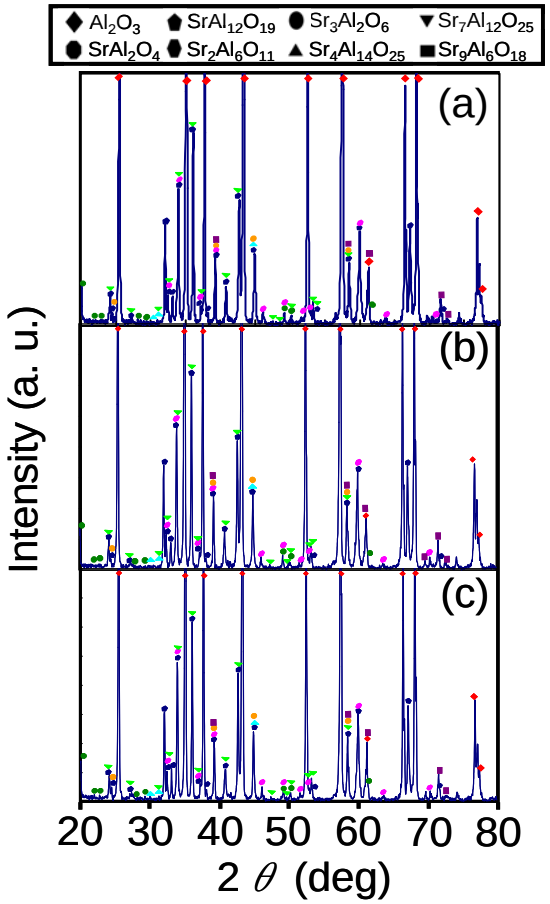


Fig. 2 XRD profiles of Sr–Al–O:$Eu^{2+}$ phosphor particles, (a)Sample 1, (b) Sample 2 and (c) Sample 3

The average crystallite diameters of the Sr–Al–O:$Eu^{2+}$ phosphor particles were estimated by Scherrer's equation from the XRD patterns at $2\theta$= 36.10º and 59.98º, which were assigned to (114) and (304), respectively, of the $SrAl_{12}O_{19}$ crystal as well as (520) and (504), respectively, of the $Sr_7Al_{12}O_{25}$ crystal. The estimated crystallite diameter sizes, which are summarized in Table II, increased with increasing sintering temperature. As a result, the values obtained at the full width at half maximum (FWHM) were assumed to represent the degrees of lattice distortion in the Sr–Al–O:$Eu^{2+}$ phosphor, grain growth, and densification in the phosphor particles obtained by elemental Al diffusion [21], [22].

The PL spectra at 300 K of the Sr–Al–O:$Eu^{2+}$ phosphor particles are shown in Fig. 3. The excitation wavelength was constant at 269 nm. All samples showed a broad violet emission peak at 405 nm, which was assigned to the f–d transition of the $Eu^{2+}$ ion. The emission intensities at 405 nm increased with increasing sintering temperature. Luminescence of the $Eu^{2+}$-doped phosphor strongly depended on the environment of the $Eu^{2+}$ ion as an emission center because of its crystal-field effect. By increasing the sintering temperature, the crystal purity of the Sr–Al–O:$Eu^{2+}$ phosphor was improved, and the distribution of $Eu^{2+}$ ions in the crystal changed from nonuniform to uniform [23]-[24]. Both $SrAl_{12}O_{19}$:$Eu^{2+}$ and $Sr_7Al_{12}O_{25}$:$Eu^{2+}$ phosphors have been reported to show violet luminescence [9], [25]. Based on the ICDD assignments, these Sr–Al–O crystals were assumed to exist in the Sr–Al–O:$Eu^{2+}$ phosphor particles because the particles were a multi-phase of various Sr–Al–O crystalline phases resulting from elemental Al diffusion. The results of XRD and PL spectroscopy at 300 K showed that the Sr–Al–O:$Eu^{2+}$ phosphor particles were neither $SrAl_{12}O_{19}$:$Eu^{2+}$ nor $Sr_7Al_{12}O_{25}$:$Eu^{2+}$ phosphors.

TABLE II
ESTIMATED CRYSTALLITE OF THE SR-AL-O:$EU^{2+}$ PHOSPHOR PARTICLES

| Sample ID | Crystallite diameter (nm) |
|---|---|
| Sample 1 | 58.7 |
| Sample 2 | 68.5 |
| Sample 3 | 109.7 |

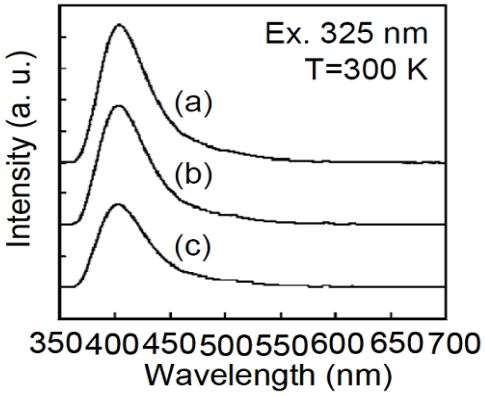


Fig. 3 PL spectra of Sr–Al–O:$Eu^{2+}$ phosphor particles at 300 K, (a) Sample 1, (b) Sample 2 and (c) Sample 3

Next, material identification by luminescence spectroscopy at low temperature was performed. Changes in the emission behavior of $Eu^{2+}$-doped phosphor at low temperature are related to transitions between energy levels of the $Eu^{2+}$ ions. The CL spectra of the Sr–Al–O:$Eu^{2+}$ phosphor particles at 85–300 K are shown in Figs. 4–6. The accelerating voltage was constant at 30 kV. All Sr–Al–O:$Eu^{2+}$ phosphor particles showed a broad emission peak at 398 nm at 300 K. By decreasing the temperature, the emission intensities at 398 nm were decreased. A new broad emission peak at 375 nm emerged at a lower temperature of 250 K, accompanied by increased intensity. This violet emission peak at 375 nm was assigned to the $^6P_{7/2}$–$^8S_{7/2}$ transition of $SrAl_{12}O_{19}$:$Eu^{2+}$. At temperatures below 200 K, the violet emission peak at around 325 nm was assumed to result from the $F^+$ center emission of α-$Al_2O_3$ [26], [27].

Katsumata et al. reported the temperature dependence of the $SrAl_{12}O_{19}$:$Eu^{2+}$ phosphor's emission properties [28]. At 310 K, the emission peak at 404 nm of our CL spectra, which was assigned to the 4f5d–$^8S_{7/2}$ transition of $SrAl_{12}O_{19}$:$Eu^{2+}$, became

dominant. Next, this dominant emission peak's position changed from 404 nm to 371 nm at 275–100 K. Furthermore, at a lower temperature of 100 K, the 371 nm emission, which was assigned to the $^6P_{7/2}$–$^8S_{7/2}$ transition of $SrAl_{12}O_{19}:Eu^{2+}$, dominated; the emission at 404 nm was not observed. The 375-nm emission peak of the Sr–Al–O:$Eu^{2+}$ phosphor particles showed behavior similar to that reported for the $SrAl_{12}O_{19}:Eu^{2+}$ at low temperature. Hence, the composition of the Sr–Al–O:$Eu^{2+}$ phosphor particles was determined to be $SrAl_{12}O_{19}:Eu^{2+}$ by the low-temperature spectroscopy.

TABLE III
ESTIMATED ACTIVATION ENERGIES OF THE SR-AL-O:$EU^{2+}$ PHOSPHOR PARTICLES

| Sample ID | Activation energy (eV) |
|---|---|
| Sample 1 | 0.037 |
| Sample 2 | 0.030 |
| Sample 3 | 0.020 |

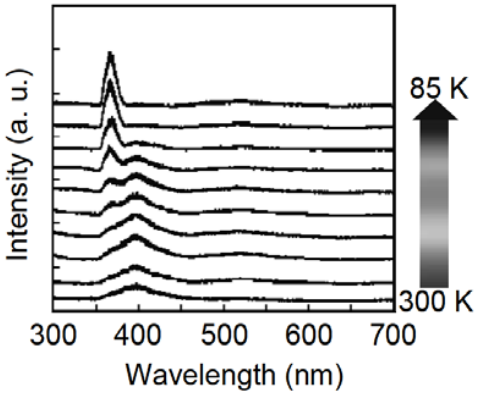


Fig. 4 CL spectra of Sample 1 at 85–300 K

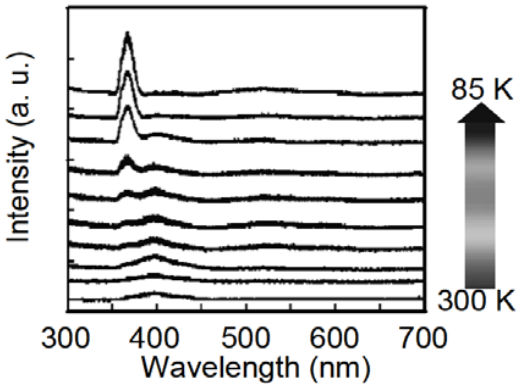


Fig. 5 CL spectra of Sample 2 at 85–300 K

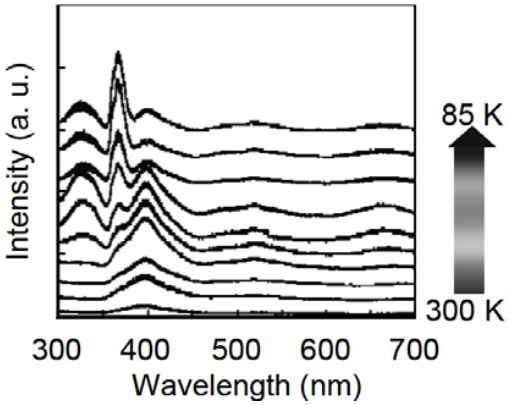


Fig. 6 CL spectra of Sample 3 at 85–300 K

Activation energies of the Sr–Al–O:$Eu^{2+}$ phosphor particles were estimated from the Arrhenius equation using the emission intensities at 398 nm obtained from each PL spectra. The activation energies of Sample 1–3 are listed in Table III and as follows: 0.037 eV for Sample 1; 0.030 eV for Sample 2; 0.020 eV for Sample 3. These values decreased with increasing sintering temperature. The variation in emission wavelength with temperature depends on the charge migration rate in a phosphor's host material [29]. For the Sr–Al–O:$Eu^{2+}$ phosphors, self-trapping holes in one $AlO_4^{5-}$ chain structure moved to the next $AlO_4^{5-}$ chain structure by hopping. Eventually, the self-trapping holes were trapped at the $Eu^{2+}$ sites in the structures, releasing the absorbed energies as luminescence. At low temperatures, the localized electron–hole pair that was created by excitation of violet light was not isolated and did not recombine. The activation energies obtained from the emission intensities' dependence on temperature corresponded to the heat energy required for holes to hop (versus the self-trapping holes in the crystal). This electron migration was closely related closely to the excited electron's transition from the $^6P_{7/2}$ level to the 4f5d level of the $Eu^{2+}$ ion. Thus, the activation energies affected the emission efficiencies of the 4f5d–$^8S_{7/2}$ transitions [30], [31]. The relationship between the crystallite diameter sizes and activation energies is shown in Fig. 7. The activation energies decreased with increasing crystallite size. In the highly crystallized $SrAl_{12}O_{19}$, the frequency of electron migration became high. In SrO–$Al_2O_3$ phase diagrams, the $SrAl_{12}O_{19}$ crystal phase can be found in the region containing over 86 mol% $Al_2O_3$ [32]. Since the elemental Al diffusion was enhanced by increasing the sintering temperature, the formation of $SrAl_{12}O_{19}$ in the Sr–Al–O:$Eu^{2+}$ phosphor particles was thus accelerated by elemental Al diffusion from the alumina particles. These results indicated that a violet $SrAl_{12}O_{19}:Eu^{2+}$ phosphor with high crystal purity was obtained by elemental Al diffusion, and the phosphor showed high emission efficiencies for 4f5d–$^8S_{7/2}$ transitions, as confirmed by the values of the activation energies.

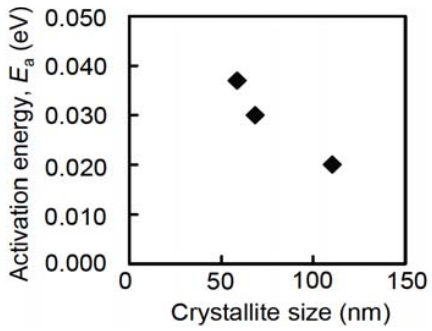


Fig. 7 Relationship between the activation energy and crystallite diameter size of Sr–Al–O:$Eu^{2+}$ phosphor particles

## IV. Conclusion

A violet Sr–Al–O:$Eu^{2+}$ phosphor was synthesized on particulate alumina from the reaction between Sr–Al–O:Eu powder and Al derived from the alumina. The violet Sr–Al–O:$Eu^{2+}$ phosphor was identified to be $SrAl_{12}O_{19}$:$Eu^{2+}$ phosphor. Although XRD measurements indicated the presence of seven types of Sr–Al–O crystals in the obtained Sr–Al–O:$Eu^{2+}$ phosphor, its emission behavior at 85–300 K under irradiation by a 30-kV accelerating voltage identified the particles as the $SrAl_{12}O_{19}$:$Eu^{2+}$ phosphor. The lower activation energy for the 4f5d–$^8S_{7/2}$ transition of the $Eu^{2+}$ ion was obtained by increasing the sintering temperature.

## References

[1] A. López, M. G. da Silva, E. Baggio-Saitovitch, A. R. Camara, R. N. Silveira Jr., and R. J. M. da Fonseca, "Luminescence of $SrAl_2O_4$:$Cr^{3+}$," J. Mater. Sci., vol.43, p. 464–468 (2008).

[2] F. Clabau, X. Rocquefelte, S. Jobic, P. Deniard, M. Whangbo, A. Garcia, and T. Le Mercier, "On the Phosphorescence Mechanism in $SrAl_2O_4$:$Eu^{2+}$ and its Co doped Derivatives," Solid State Sci., vol. 9, p.608–612 (2007).

[3] Y. Xu, Y. He, and X. Yuan, "Preparation of Nanocrystalline $Sr_3Al_2O_6$ Powders Via Citric Acid Precursor," Powder Tech., p.172, 99–102 (2007).

[4] P. Page, R. Ghildiyal, and K.V.R. Murthy, "Synthesis, Characterization and Luminescence of $Sr_3Al_2O_6$ Phosphor with Trivalent Rare Earth Dopant," Mater. Res. Bull., vol. 41, p.1854–1860 (2006).

[5] Y. Lin, Z. Tang, and Z. Zhang, "Preparation of Long-afterglow $Sr_4Al_{14}O_{25}$-based Luminescent Material and its Optical Properties," Mater. Lett., vol. 51, p. 14–18 (2001).

[6] Y. Jia, M. Yei, and W. Jia, "Stress-Induced Mechanoluminescence in $SrAl_2O_4$:$Eu^{2+}$,$Dy^{3+}$," Opt. Mater., vol. 28, p. 974–979 (2006).

[7] Y. Zhu, M. Zheng, J. Zeng, Y. Xiao, and Y. Liu, "Luminescence Enhancing Encapsulation for Strontium Aluminate Phosphors with Phosphate," Mater. Chem. Phys., vol. 113, p. 721–726 (2009).

[8] P. Dorenbos, "Energy of the First $4f^7 \rightarrow 4f^6 5d$ Transition of $Eu^{2+}$ in Inorganic Compounds," J. Lumin., vol. 104, p.239–260 (2003).

[9] H. Akasaka, H. Tada, T. Ooki, A. Nakamura, K. Komatsu, S. Tsuchida, S. Ohshio, N. Nambu, and H. Saitoh, "New Violet Phosphor $Sr_7Al_{12}O_{25}$:$Eu^{2+}$ Synthesized from Sr–Al–O:Eu Powder Mounted on Polycrystalline Alumina," Jpn. J. Appl. Phys., vol. 49, 122601 (2010).

[10] N. Tanaka, S. Ohshio, H. Saitoh, K. Uematsu, "Crystal growth of highly oriented zinc oxide by laser deposition technique with metal-EDTA complexes", Jpn. J. Appl. Phys., vol. 37 (10A), L1165-L1168 (1998).

[11] Hiroki Akasaka, Masahiro Ohto, Yasuhiro Hasebe, Atsushi Nakamura, Shigeo Ohshio, Hidetoshi Saitoh, "Yttria coating synthesized by reactive flame spray process using Y-EDTA complex", Surf. Coat. Tech., vol. 205 (13-14), p. 3877-3880 (2011).

[12] N. Tanaka, H. Wakabayashi, S. Mochizuki, S. Ohshio, H. Saitoh, "Synthesis of Y-B-C-O films with EDTA complexes assisted by eximer laser ablation", J. Mater. Res., vol. 13 (11), p. 2775-2778 (1998).

[13] K. Komatsu, S. Tsuchida, H. Maruyama, A. Nakamura, S. Ohshio, H. Akasaka, and H. Saitoh, "Synthesis of a Violet Sr–Al–O:$Eu^{2+}$ Phosphor Particle Using Elemental Al Diffusion," Int. J. Appl. Ceram. Technol., vol. 1-8, 12050 (2012).

[14] M. Kučera and J. Novák, "Radiative-Recombination Transitions in Sulphur-Doped GaSb," J. Lumin., vol. 129, p. 238–242 (2009).

[15] F. Zhang, S. Chen, J. F. Chen, H. L. Zhang, J. Li, X. J. Liu, and S. W. Wang, "Characterization and Luminescence Properties of AlON:$Eu^{2+}$ Phosphor for White-Emitting-Diode Illumination," J. Appl. Phys., vol. 111, 083532 (2012).

[16] S. Zhang, Y. Nakai, T. Tsuboi, Y. Huang, and H. J. Seo, "Luminescence and Microstructural Features of Eu-Activated $LiBaPO_4$ Phosphor," Chem. Mater., vol. 23, p. 1216–1224 (2011).

[17] X. Zhiguo, S. Jiayue, L. Libing, and D. Haiyan, "Phase Structure and Temperature Dependent Luminescence Properties of $Sr_2LiSiO_4F$:$Eu^{2+}$ and $Sr_2MgSi_2O_7$:$Eu_{2+}$ Phosphors," J. Rare Earths, vol. 28, p. 874–877 (2010).

[18] Z. Yanfang, L. Lan, Z. Xiaosong, and X. Qun, "Temperature Effects on Photoluminescence of YAG:$Ce^{3+}$ Phosphor and Performance in White Light-Emitting Diodes," J. Rare Earths, vol. 26, p. 446–449 (2008).

[19] P. A. Rodnyi, A. N. Mishin, S. B. Mikhrin, and A. S. Potapov, "Temperature-Induced Variation of the Emission Band Intensities of an $SrAl_{12}O_{19}$:Pr Phosphor," Tech. Phys. Lett., vol. 28, p. 991–993 (2002).

[20] H. Najafov, S. Tokita, S. Ohshio, A. Kato, and H. Saitoh, "Green and Ultraviolet Emissions From Anatase $TiO_2$ Films Fabricated by Chemical Vapor Deposition," Jpn. J. Appl. Phys., vol. 44, p. 245–253 (2005).

[21] A. D. Deshmukh, S. J. Dhoble, and N.S. Dhoble, "Optical Properties of $MAl_{12}O_{19}$:Eu (M = Ca, Ba, Sr) Nanophosphors," Adv. Mat. Lett., vol. 2, 38–42 (2011).

[22] R. Chen, Y. Wang, Y. Hu, Z. Hu, and C. Liu, "Modification on Luminescent Properties of $SrAl_2O_4$:$Eu^{2+}$,$Dy^{3+}$ Phosphor by $Yb^{3+}$ Ions Doping," J. Lumin., vol. 128, p. 1180–1184 (2008).

[23] S.-S. Yao, L.-H. Xue, Y.-W. Yan, Y.-Y. Li, and M.-F. Yan, "Luminescent characteristics of $Sr_2ZnSi_2O_7$ : $Eu^{3+}$ phosphor for ultraviolet light emitting diodes," J. Ceram. Process. Res., vol. 11, p. 669–672 (2010).

[24] H. M. H. Fadlalla, C. C. Tang, E.M. Elssfah, J. Zhang, E. Ammar, J. Lin, and X. X. Ding, "Synthesis and Characterization of Photoluminescent Cerium-doped Yttrium Aluminum Garnet," Mater. Res. Bull., vol. 43, p. 3457–3462 (2008).

[25] V. Singha, T. K. G. Rao, and J.-J. Zhu, "Preparation, Luminescence and Defect Studies of $Eu^{2+}$-activated Strontium Hexa-aluminate Phosphor Prepared via Combustion Method," J. Solid State Chem., vol. 179, p. 2589–2594 (2006).

[26] G. Pezzotti, M. C. Munisso, A. A. Porporati, and K. Lessnau, "On the Role of Oxygen Vacancies and Lattice Strain in the Tetragonal to Monoclinic Transformation in Alumina/Zirconia Composites and Improved Environmental Stability," Biomaterials, vol. 31, p. 6901–6908 (2010).

[27] B. G. Draeger and G.P. Summers, "Defects in Unirradiated α-$Al_2O_3$," Phys. Rev. B., vol. 19, p. 1172–1177 (1979).

[28] T. Katsumata, Y. Kohno, H. Kubo, S. Komuro, and T. Morikawa, "Low Temperature Fluorescence Thermometer Application of Long Afterglow Phosphorescent $SrAl_{12}O_{19}$:$Eu^{2+}$,$Dy^{3+}$ Crystals," Rev. Sci. Instrum., vol. 76, 084901 (2005).

[29] M. Yamaga, Y. Tanii, N. Kodama, T. Takahashi, M, Honda, and N. Kodama, "Mechanism of Long-Lasting Phosphorescence Process of $Ce^{3+}$-doped $Ca_2Al_2SiO_7$ Melilite Crystals," Phys. Rev. B., vol. 65, 235108 (2002).

[30] M. Wang, Xia Zhang, Z. Hao, X. Ren, Y. Luo, X. Wang, and J. Zhang, "Enhanced Phosphorescence in N Contained $Ba_2SiO_4$:$Eu^{2+}$ for X-ray and Cathode Ray Tubes," Opt. Mater., vol. 32, p. 1042–1045 (2010).

[31] Y. Zhang, L. Li, X. Zhang, and Q. Xi, "Temperature Effects on Photoluminescence of YAG:$Ce^{3+}$ Phosphor and Performance in White Light-emitting Diodes," J. Rare Earths., vol. 26, p. 446–449 (2008).

[32] X. Ye, W. Zhuang, J. Wang, W. Yuan, and Z. Qiao, "Thermodynamic Description of SrO-$Al_2O_3$ System and Comparison with Similar Systems," J. Phase Equilibria. Diffus., vol. 28, p. 4 (2007).

**K Komatsu** was born in Japan in 1985. He received doctoral degree at Nagaoka University of Technology in 2013. He is a postdoctoral fellow researcher in Nagaoka University of Technology. His major study filed is inorganic materials/physical properties, such as functional oxides phosphor materials.

**H. Maruyama** was received master degree at Nagaoka University of Technology. He graduated the Nagaoka University of Technology in 2009.

**A. Kato** was received doctoral degree at Kyoto University in 1998. He is an associate Professor in Nagaoka University of Technology. His research themes are optical properties of rare-earth compounds.

**A. Nakamura** was received doctoral degree at Nagaoka University of Technology. He is with the Chubu Chelest Co., Ltd. and he is also with the Nagaoka Univeristy of Technology as visiting associate professor. His major study filed is inorganic materials/physical properties.

**S. Ohshio** is a technical specialist at Nagaoka University of Technology. His major field studies are science education and inorganic materials/physical properties

**H. Akasaka** was with the Nagaoka Univeristy of Technology. He received doctoral degree at Tokyo Institute of Technology in 2007. He is an associate professor in Tokyo Institute of Technology. His major study filed is inorganic materials/physical properties.

**H. Saitoh** was received doctoral degree at Nagaoka University of Technology in 1990. He is a professor in Nagaoka University of Technology. His research themes are crystal growth of thin films, crystal growth of thin films, material design of superhard compound, material design of superhard compound, and opto ceramic materials, opto ceramic materials.